# On modelling hydraulic fractures in inhomogeneous media

Liliana Rybarska-Rusinek Dawid Jaworski Ewa Rejwer Aleksandr Linkov
rybarska@prz.edu.pl

**Abstract**

Hydraulic fracturing is commonly performed in rock stratum composed of layers and structural blocks and containing other inhomogeneities like inclusions, pores and cracks. The purpose of the work is to develop methods facilitating accurate, stable and robust evaluation of the stresses in strongly inhomogeneous medium with propagating hydraulic fracture. The paper presents authors results, obtained to reach this goal by using: special forms of hypersingular boundary integral equations (H-BIE), solved by the boundary element methods (BEM); higher order approximations of the boundary and densities; tip and (multi-) wedge elements; efficient analytical evaluation of influence coefficients and multipole moments; and combination of H-BEM with fast multipole methods.

## 1 Introduction

Hydraulic fracturing is commonly performed in rock stratum composed of layers and structural blocks and containing other inhomogeneities like inclusions, pores and cracks. Meanwhile, to the date, the inhomogeneous structure of rock is either not accounted for, or only horizontal layers are considered, while the fracture is assumed to propagate in the vertical plane (see, e.g. reviews [1], [12]). Our objective is to develop computational techniques applicable to much wider range of structures. To reach the goal we use the *hypersingular* boundary integral equations (H-BIE), which present a natural means to capture both discontinuities on contacts of structural elements and also singular behaviour of stresses at common apexes of blocks and at fracture contours. We employ those forms of the H-BIE and the boundary element methods (BEM), which are tailored for blocky structures. Since accounting for inhomogeneities requires special attention to the accuracy, we employ (i) higher order approximations of the densities, (ii) special tip and (multi-) wedge elements and (iii) recurrent analytical evaluation of all influence coefficients and all the multipole moments. Combination of the H-BEM with the fast multipole method (FMM) serves us to consider strongly inhomogeneous systems, for which the number of degrees of freedom (DOF) may exceed million. The paper presents authors findings in implementing these approaches. Both 2D and 3D problems are considered. The exposition is illustrated by the results of numerical tests, which confirm efficiency of the methods developed.

## 2 CV hypersingular equation for 2D problems

### 2.1 Basic complex variable integrals

For 2D problems, it is reasonable to employ the advantages of complex variables (CV). The needed CVH-BEM for blocky systems with non-ideal contacts, cracks, inclusions, pores and other inhomogeneities may be found elsewhere (see, e.g. [8], [13]). It appears that actually only six standard integrals are to be evaluated when solving this BIE by the CVH-BEM. Moreover, it is sufficient to focus on two integrals, singular and hypersingular, respectively:

$$\int\limits_{L_e} \frac{f(\tau)}{\tau - t} d\tau, \ \int\limits_{L_e} \frac{f(\tau)}{(\tau - t)^2} d\tau, \tag{1}$$

where $L_e$ is a boundary element, $f(\tau)$ is the density function, $t = x + iy$ is the CV coordinate of a field point and $\tau$ is the CV coordinate of an integration point. The remaining integrals are proper and they are promptly evaluated when having the integrals (1).

## 2.2 Approximation of the contour and the density function

i) *Contour approximation by straight and circular-arc boundary elements*

With purpose to increase the accuracy of approximation of a contour, we represent it by combination of circular-arc and, when appropriate, straight boundary elements. The radii of neighbouring elements are prescribed in a way, which provides continuity of the tangent at common points of elements on any smooth part of the contour. To make the path of integration standard, we transform a circular-arc (straight) element into the standard circular-arc (straight) element of unit radius (half-length). To this end, we use the linear transformation of the CV coordinates:

$$\tau = \tau_c + A \exp{(i\alpha_c)}\tau', \tag{2}$$

where $\tau_c$ is the CV global coordinate of the center of a circular-arc (straight) element; $A = -iR$ for a circle of radius $R$, $A = l$ for a straight element of the length $2l$; $\alpha_c$ is the angle between the tangent at the element midpoint and the global $x$-axis. The standard circular-arc (straight) element is located symmetrically with respect to the local axis $x'$ $(y')$.

ii) *Approximation of the density function*

The density function on the standard element is approximated in the following way:

$$f(\tau') = \left(\tau' - c'\right)^{\beta} P\left(\tau'\right), \tag{3}$$

where $c'$ is the end point of the integration path; $P(\tau')$ is a linear combination of form functions. The form functions for the standard circular-arc (straight) element are trigonometric (algebraic) Lagrange polynomials of an arbitrary order. For an ordinary (non-singular) element, we have $\beta = 0$. For tip, corner and multi-wedge elements, the exponent $\beta$ in (3) accounts for power-type asymptotics of the density. Without loss of generality, we assume that $|\beta| < 1$. The value of $\beta$ is found numerically by using a subroutine, which employs the method suggested in [3], [9]. We neglect the imaginary part of $\beta$ in a case, when $\beta$ is not real, and we represent the absolute value of its real part as a rational fracture $|\beta| = \frac{m}{n}$; $m < n$. Normally, it is sufficient to use the polynomials $P\left(\tau'\right)$ of the second order and to take $n$ and $m$ less than 10.

The integrals (1) are evaluated recurrently for the degrees of $\tau'$ entering the polynomials $P\left(\tau'\right)$ (see, e. g. [8]). The starting integrals are [9]:

$$S_0 = \int\limits_b^c \frac{\tau^\beta}{\tau - t} d\tau = \begin{cases} \frac{1}{\beta}\left(c^\beta - b^\beta\right) + \sum\limits_{s=0}^{n-1} t_s^m Ln \frac{\sqrt[n]{c} - t_s}{\sqrt[n]{b} - t_s} + \pi i t_0^m \delta_t, & \beta \geqslant 0 \\ \sum\limits_{s=0}^{n-1} t_s^{-m} Ln \frac{\sqrt[n]{c} - t_s}{\sqrt[n]{b} - t_s} + \pi i t_0^{-m} \delta_t, & \beta < 0 \end{cases}, \tag{4}$$

$$I_0 = \int_b^c \frac{\tau^\beta}{(\tau - t)^2} d\tau = \begin{cases} \frac{\beta}{t} S_0 - \frac{c^\beta}{c-t} + \frac{b^\beta}{b-t} - \frac{1}{t}\left(c^\beta - b^\beta\right), & \beta \geqslant 0 \\ \frac{\beta}{t} S_0 - \frac{c^\beta}{c-t} + \frac{b^\beta}{b-t}, & \beta < 0 \end{cases}, \tag{5}$$

where $\delta_t = 1$ for $t \in [b,c]$, $\delta_t = 0$ for $t \notin [b,c]$ and $t = |t| \exp(i\gamma)$ and $t_s = |t|^{\frac{1}{n}} \exp\left(i\left(\gamma + 2s\pi\right)/n\right)$ is a root of the complex value $t$. The roots $\sqrt[n]{b}$ and $\sqrt[n]{c}$ are principal ones ($s = 0$).

## 2.3 The FMM-BEM. Recurrent formulae for multipole moments

As mentioned, when considering strongly inhomogeneous structures, we need to solve problems with many DOF. The efficient approach to solving large scale problems (with up to millions of DOF) consists in combining the BEM with the FMM. The main ideas and detailed explanations of the FMM may be found elsewhere (e.g. [6], [11]). Its application to blocky systems with cracks, inclusions and pores has been started in [13]. Not dwelling on building the hierarchical tree, discussed in [13], we focus on recurrent evaluation of multipole moments in the complex variables. For certainty, we consider the Laplace equation with the fundamental solution $-\frac{1}{2\pi k} \ln|t - \tau|$, where $k$ is the conductivity at a considered region of a medium. The function $U_l(t,\tau) = -\frac{1}{2\pi k} \ln(t - \tau)$, when expanded into the Taylor's series at a point $\tau_0$, is represented as (e.g. [11]):

$$U_l(t,\tau) = \frac{1}{2\pi k} \sum_{l=0}^{\infty} O_l(t - \tau_0) I_l(\tau - \tau_0), \tag{6}$$

where $O_0(t - \tau_0) = -Ln(t - \tau_0)$, $O_l(t - \tau_0) = \frac{(l-1)!}{(t-\tau_0)^l}$ for $l \geqslant 1$, $I_l(\tau - \tau_0) = \frac{(\tau-\tau_0)^l}{l!}$ for $l \geqslant 0$. The kernel functions for the integrals (1) are then prescribed as the derivatives of $U_l$:

$$J_S(t,\tau) = k\frac{\partial U_l(t,\tau)}{\partial t} = \frac{1}{2\pi} \sum_{l=0}^{\infty} \left(-O_{l+1}(t - \tau_0)\right) I_l(\tau - \tau_0), \tag{7}$$

$$J_H(t,\tau) = k^2 \frac{\partial U_l(t,\tau)}{\partial \tau \partial t} = \frac{k}{2\pi} \sum_{l=1}^{\infty} \left(-O_{l+1}(t - \tau_0)\right) I_{l-1}(\tau - \tau_0). \tag{8}$$

Thus, the real parts of the integrals (1) are presented in the following forms:

$$Re\left(\int_{L_e} \frac{f(\tau)}{\tau - t} d\tau\right) =$$

$$= \frac{1}{2\pi} Re\left(-O_1(t - \tau_0) \int_{L_e} f(\tau) d\tau + \sum_{l=1}^{l_m} \left(-O_{l+1}(t - \tau_0)\right) \int_{L_e} f(\tau) I_l(\tau - \tau_0) d\tau\right), \tag{9}$$

$$Re\left(\int_{L_e} \frac{f(\tau)}{(\tau - t)^2} d\tau\right) = \frac{1}{2\pi} Re\left(\sum_{l=1}^{l_m} \left(-O_{l+1}(t - \tau_0)\right) \int_{L_e} f(\tau) I_{l-1}(\tau - \tau_0) d\tau\right). \tag{10}$$

The integrals on the right-hand side of (9) and (10) are called multipole moments of order $l$; $l_m$ is the highest degree of multipole moments used in the expansions.

It can be seen that, when using the approximation (3), evaluation of multipole moments is reduced to considering the standard integral of the form:

$$M_j^l = \int_{b'}^{c'} \tau'^j \left(\tau' - c'\right)^\beta \left(\tau' - \tau_0'\right)^l d\tau', \tag{11}$$

where $b'$ and $c'$ is start and end point of a standard boundary element in its local coordinates, respectively. For a three-node approximation of a density, $j = 0, 1, 2$ when considering the standard straight element; $j = -2, -1, 0$ when an element is the standard circular-arc element. The values $M_j^l$ may be called the *standard multipoles* of order $l$.

In order to obtain analytical recurrence formulae for them, when the element is straight, we firstly consider the integrals:

$$J^l = \int_{b'}^{c'} \left(\tau' - c'\right)^\beta \left(\tau' - \tau_0'\right)^l d\tau'. \tag{12}$$

Analytical evaluation of the starting integral $J^0$, being obvious, the integrals (12) for $l \geqslant 1$ are evaluated recurrently. Specifically, for $\beta \geqslant 0$, we have:

$$J^l = M_0^l = \frac{l\left(c' - \tau_0'\right)}{l+1+\beta} J^{l-1} - \frac{\left(b' - c'\right)^{\beta+1}\left(b' - \tau_0'\right)^l}{l+1+\beta}. \tag{13}$$

Similarly, for $\beta \leqslant 0$, we have:

$$J^l = M_0^l = \frac{l\left(c' - \tau_0'\right)}{l+1-\beta} J^{l-1} - \frac{\left(b' - c'\right)^{1-\beta}\left(b' - \tau_0'\right)^l}{l+1-\beta}. \tag{14}$$

Then the multipoles for the standard *straight* (ordinary or singular multi-wedge) element are found from the relations:

$$M_0^l = J^l,\ M_1^l = J^{l+1} + \tau_0' J^l,\ M_2^l = J^{l+2} + 2\tau_0' J^{l+1} + \tau_0^{2\prime} J^l. \tag{15}$$

For the standard circular-arc element, the starting integrals are:

$$M_{-1}^0 = \int_{b'}^{c'} \frac{\left(\tau' - c'\right)^\beta}{\tau'} d\tau',\ M_{-2}^0 = \int_{b'}^{c'} \frac{\left(\tau' - c'\right)^\beta}{\tau'^2} d\tau'. \tag{16}$$

They are found analytically by using formulae (4).

Then the multipoles for the standard *circular-arc* (ordinary or singular multi-wedge) element are obtained by employing the recurrent rules:

$$M_0^l = J^l,\ M_{-1}^l = J^{l-1} - \tau_0' M_{-1}^{l-1},\ M_{-2}^l = M_{-1}^{l-1} - \tau_0' M_{-2}^{l-1}, \tag{17}$$

where $J^l$ are defined above by equations (13) and (14).

## 3 Numerical example

As an example, we consider a plane harmonic problem for a steady flow of heat (electric current, ground water) in a medium containing many thin impermeable straight barriers (insulators). The medium without the barriers is isotropic with the conductivity $k_0$. For certainty and brevity, we shall discuss a heat flow and call the barriers "cracks". Assume that the cracks have the same length $2l$, while their orientation angle $\alpha$ is randomly distributed in the interval $[0, \pi]$ with the uniform distribution function. Therefore, macroscopically the medium is isotropic and it is characterized by the scalar value of the effective conductivity $k$. Our purpose is to calculate the effective conductivity as a function of the crack density $\rho$. The latter is defined as

$$\rho = \frac{2}{\pi} \frac{N(2l)^2}{A},$$

where $A$ is the area of a representative volume element (RVE), $N$ is the number of cracks in it.

For certainty, we assume the RVE to be a square with the side $L$. For the square RVE, $A = L^2$. The square is large enough to include a sufficient number of cracks to represent the effective conductivity to an accepted tolerance. Below we shall use different values of the number $N$ to see how it influences the convergence to the limit, giving the effective conductivity.

Naturally, the size of the RVE depends also on the crack concentration. We assume that the centers of cracks are randomly distributed in the square with the uniform distribution function. To exclude intersection of cracks for high concentrations, we randomly seed their centers on the multiplicity of the centers of the $\sqrt{N} \times \sqrt{N}$ square mesh and take $2l$ not exceeding $L/\sqrt{N}$. According to the density definition, the limiting case $2l = L/\sqrt{N}$ corresponds to the concentration $\rho = 2/\pi = 0.637$. We have performed calculations in the range of the density $[0, 0.61]$. Examples of the RVE with randomly seeded cracks are given in Figure 1.

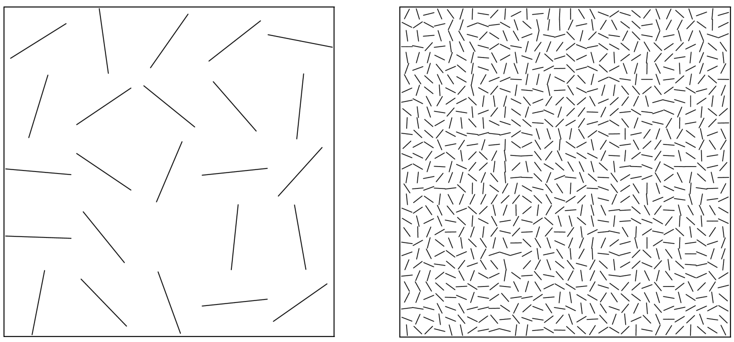

Figure 1: Representative volume element with a) $N = 25$; b) $N = 900$ cracks.

We prescribe zero flux on the horizontal sides of the RVE and constant values $T_1$ and $T_2$ of the temperature on the left and right vertical side, respectively. Without loss of generality, we may consider the difference $T_1 - T_2$. Therefore we may set $T_2 = 0$. The cracks being insulators, the flux is zero, while the temperature is discontinuous across a crack. When normalizing the temperature by $T_1$, the crack length and coordinates by $L$, and the flux by $k_0 T_1/L$, we arrive at the homogenization problem for the square RVE of the unit size. Its horizontal sides are insulated; its left vertical side is subjected to the unit temperature; it right vertical side has zero temperature. The effective conductivity is normalized by $k_0$.

In the normalized values, the normalized effective conductivity is $k = Q_i$, where $Q_i$ is the total flux through the left ($i = 1$) or right ($i = 2$) vertical side of the unit RVE. The ratio $(Q_1 - Q_2)/Q_1$ characterizes the relative error of numerical calculations.

We estimated the tolerance, to which the effective conductivity is simulated, by prescribing various number $N$ of cracks in the unit RVE for each of the considered crack densities. Specifically, we took $N = 25$, 100, 400 and 900. The densities were $\rho = 0.0$, 0.1, 0.21, 0.31, 0.41, 0.51, 0.61.

In numerical calculations, we solved the complex variable H-BIE, suggested in [5], by using the CV-BEM and the FMM with the recurrent evaluation of the moments as explained above. The mesh and approximations on the boundary elements (BE) were as follows. Each side of the unit RVE was represented by equal BE. Their size was taken less than the minimal distance $1/\sqrt{N}$ between the crack centers; it was equal to $1/25 = 0.04$ for $N = 25$, and $1/65 = 0.0154$ for $N = 900$. Each crack was represented by four elements, two ordinary and two tip; the tip elements accounted for the square-root asymptotics of the temperature discontinuity near the crack tips. All the elements (ordinary and tip) were three-node elements, employing polynomials of the second order for the density approximation. The maximal order of the algebraic system was near 12000 for the maximal number of cracks $N = 900$.

The parameters of the FMM were chosen on the basis of analytical estimations complimented with specially designed numerical experiments. It was established that to obtain sufficiently accurate results, the number of BE in a leaf may be taken 5 for $N = 25$, and 10 for $N = 900$. The reasonable number of terms, held in the multipole expansions, is 18. With these parameters, the time of calculations on a conventional laptop does not exceed 1200 seconds for the maximal number of cracks $N = 900$.

Figure 2a presents the dependence of the effective conductivity on the crack concentration for various numbers N of cracks in the RVE. It clearly shows that with the growth of the concentration, the mutual interaction between cracks grows, so that greater number of cracks is required to reproduce the effective conductivity to a prescribed tolerance. Specifically, for the maximal density $\rho = 0.61$, the tolerance of 0.5% is guaranteed when $N \geqslant 400$.

It is interesting to compare the numerical results obtained to this tolerance with the equation, suggested by Hoenig [7]. In terms of the normalized conductivity, the Hoenig equation is $k = \frac{9}{9+8\rho}$. The comparison of our results with the Hoenig equation is given in Figure 2b. It appears that for $\rho \geqslant 0.2$, the Hoenig's equation is indeed applicable, although to the tolerance not exceeding 5%.

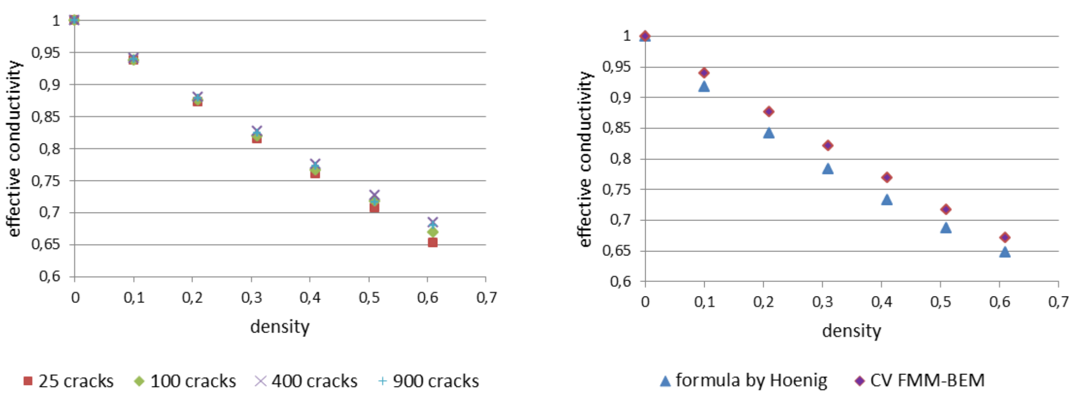


Figure 2: a) the effective thermal conductivity; b) the comparison with the Hoenig formula.

# 4 Hypersingular equation for 3D problems

## 4.1 Basic integrals

We employ the same means to increase the accuracy, which have been employed in 2D problems. Specifically, we use higher order polynomial approximations and account for the asymptotic behavior of a density near the contour of a fracture.

Consider a system of 3D isotropic elastic blocks. For simplicity, we assume that the Poisson's ratio is the same for all the blocks. This assumption is acceptable for most of rocks having the Poisson's ratio $\nu$ close to 0.3. Then the real H-BIE for blocky systems with cracks, inclusions and pores is (see e.g. [8]):

$$\int\limits_S \left( \frac{1}{4\mu^+} J_S^+ (x,\xi)\, t_n^+ - \frac{1}{4\mu^-} J_S^- (x,\xi)\, t_n^- \right) dS_\xi - \int\limits_S \frac{1}{4\mu} J_H (x,\xi)\, \Delta u (x,\xi)\, dS_\xi =$$

$$= \frac{1}{2} \left( \frac{1}{4\mu^+} t_n^+ (x) + \frac{1}{4\mu^-} t_n^- (x) \right). \tag{18}$$

Herein, $S$ is the total surface of blocks; the superscript " + " (" − ") refers to the limit of a value from the side, with respect to which the normal $n$ is outward (inward); $\mu$ is the shear modulus; $t_n$, $\Delta u$ is the vector of the tractions and the displacement discontinuities (DD), respectively. The matrix $J^S$ is obtained by applying the traction operator $T_n$ to the matrix of fundamental solutions $U$:

$$J_{ik}^S = (T_n U)_{ik} = 2\mu \left[ \frac{\nu}{1-2\nu} \frac{\partial U_{jk}(x,y)}{\partial x_j} n_i + \frac{1}{2} \left( \frac{\partial U_{ik}(x,y)}{\partial x_j} + \frac{\partial U_{jk}(x,y)}{\partial x_i} \right) n_j \right]. \tag{19}$$

The hypersingular kernel $J_H(x,\xi)$ is defined as $J^H(x,y) = T_n \left( J^S(x,y) \right)^T$. For infinite elastic medium, the matrix $U(x,y)$ of fundamental solutions is defined by the Kelvin's solution:

$$U_{ik}(x,y) = \frac{1}{16\pi\mu(1-\nu)} \left[ (3-4\nu)\frac{\delta_{ik}}{R} + \frac{(x_i-y_i)(x_k-y_k)}{R^3} \right], \tag{20}$$

where $R = \sqrt{(x_i-y_i)^2}$, $i = 1,2,3$, is the distance between the field $x$ and integration $y$ points. Then

$$J_{ik}^S = \frac{1}{8\pi(1-\nu)} \left[ 2\nu \frac{\partial \frac{1}{R}}{\partial x_k} n_i + 2(1-\nu) \left( \frac{\partial \frac{1}{R}}{\partial x_i} n_k + \delta_{ik} \frac{\partial \frac{1}{R}}{\partial x_j} n_j \right) - \frac{\partial^3 R}{\partial x_j \partial x_i \partial x_k} n_j \right], \tag{21}$$

$$J_{ik}^H = n_j^x S_{ijk} = n_j^x \frac{\mu}{4\pi(1-\nu)} \left\{ n_s \frac{\partial^4 R}{\partial x_i \partial x_j \partial x_k \partial x_s} - \left[ 2\nu \left( n_k \frac{\partial^2}{\partial x_i \partial x_j} + \delta_{ij} n_s \frac{\partial^2}{\partial x_k \partial x_s} \right) + \right.\right.$$

$$\left.\left. +(1-\nu) \left( n_i \frac{\partial^2}{\partial x_j \partial x_k} + n_j \frac{\partial^2}{\partial x_i \partial x_k} + \delta_{ik} n_s \frac{\partial^2}{\partial x_j \partial x_s} + \delta_{jk} n_s \frac{\partial^2}{\partial x_i \partial x_s} \right) \right] \frac{1}{R} \right\}. \tag{22}$$

When solving a problem by the BEM, we need to evaluate integrals with these kernels over a BE.

### 4.2 Approximation of the contour and density

We solve the H-BIE (18) by the BEM. To increase the accuracy of approximation of the surface $S$, we represent it by the sum of $p$, in general curvilinear, triangular elements $S^q$ $(q = 1, 2, \dots, p)$. For each of the triangles, we assign the plane through its three vertices and the plane triangle in this plane. Integration over a curvilinear triangle is performed by transforming it into the plane triangle by using common shape-functions (see, e.g. [2]). Similar to 2D problems, we assume an element to be small enough to make second order approximations of the boundary accurate enough. Thus the shape functions are second order polynomials in the local coordinates of the plane triangle. The surface Jacobean is expanded into Taylor series in these coordinates. For further discussion its order does not matter. In practical calculations, for a small triangle, it is sufficient to use polynomials of the second order. Each plane triangle may be represented as a sum of two right triangles. Consequently, it is sufficient to consider a plane right triangle. With these prerequisites, it is possible to evaluate all the integrals entering (18) over a curvilinear triangle analytically when the tractions are approximated by polynomials, while the DD are approximated by polynomials multiplied by a weight function. The latter is the unit for triangles not adjusting to the fracture contour; it equals to square-root of the distance $d$ from the fracture contour for triangles having at least one apex located on the contour. When deriving the quadrature rules for triangles with these approximations, we follow the line of the paper [10]. We extend the results of this paper to singular integrals with polynomial density and to hypersingular integrals with the density accounting for the square-root asymptotics near the fracture contour.

*Singular integrals*

Singular integrals contain the tractions as the density vector. Commonly, the tractions are non-singular and they may be accurately approximated by polynomials. Then evaluation of singular integrals is reduced to finding the partial derivatives $\frac{\partial}{\partial x_1}, \frac{\partial}{\partial x_2}, \frac{\partial}{\partial x_3}$ of the function:

$$A^{kl}(x_2, x_3) = \int\limits_{T^q} \frac{(x_3 - y_2)^l\,(x_3 - y_2)^k}{\sqrt{x_1^2 + (x_2 - y_2)^2 + (x_3 - y_3)^2}} dS_y, \tag{23}$$

where $T^q$ is a right triangle, the $x_1$-axis is normal to the triangle plane, the $x_2$-axis is along the side of the length $a$; the $x_3$-axis is along the side of the length $b$; the directions of $y_i$ are those of $x_i$ $(i = 2, 3)$. Conversion to iterated integrals yields:

$$A^{kl}(x_2, x_3) = \int\limits_{x3-b}^{x_3} \eta^l \left( \int\limits_{\alpha+\beta\eta}^{x_2} \frac{\xi^k}{\sqrt{x_1^2 + \xi^2 + \eta^2}} d\xi \right) d\eta, \tag{24}$$

where $\xi = x_2 - y_2,\ \eta = x_3 - y_3,\ \alpha = x_2 - a + \frac{a}{b}x_3,\ \beta = -\frac{a}{b}$.

For the integral on the r.h.s. of (24) we have the recurrence formulae:

$$A^{kl} = \int\limits_{x_3-b}^{x_3} \eta^l \left[ \frac{1}{k}\xi^{k-1}\sqrt{x_1^2 + \xi^2 + \eta^2} \right]_{\xi=\alpha+\beta\eta}^{\xi=x_2} d\eta - \frac{k-1}{k} x_1^2 A^{(k-2)l} - \frac{k-1}{k} A^{(k-2)(l+2)},$$

where

$$A^{1l} = \int\limits_{x_3-b}^{x_3} \eta^l \left[ \sqrt{x_1^2 + \xi^2 + \eta^2} \right]_{\alpha+\beta\eta}^{x_2} d\eta, \tag{25}$$

$$A^{0l} = \int\limits_{x_3-b}^{x_3} \eta^l \left[ ln \left| \xi + \sqrt{x_1^2 + \xi^2 + \eta^2} \right| \right]_{\alpha+\beta\eta}^{x_2} d\eta. \tag{26}$$

This implies that, we need to evaluate four integrals only:
$J_1^s = \int\limits_{x_3-b}^{x_3} \eta^s \sqrt{x_1^2 + x_2^2 + \eta^2} d\eta,$
$J_2^s = \int\limits_{x_3-b}^{x_3} \eta^s \sqrt{x_1^2 + (\alpha + \beta\eta)^2 + \eta^2} d\eta,$
$J_3^s = \int\limits_{x_3-b}^{x_3} \eta^s \ln \left| x_2 + \sqrt{x_1^2 + x_2^2 + \eta^2} \right| d\eta,$
$J_4^s = \int\limits_{x_3-b}^{x_3} \eta^s \ln \left| (\alpha + \beta\eta) + \sqrt{x_1^2 + (\alpha + \beta\eta)^2 + \eta^2} \right| d\eta.$

The first two of them are found by using the recurrence equation:

$$I^n = \int \frac{\eta^n}{\sqrt{A\eta^2 + B\eta + C}} d\eta$$

$$= \frac{\eta^{n-1}}{nA} \sqrt{A\eta^2 + B\eta + C} - \frac{\left(n - \frac{1}{2}\right) B}{nA} I^{n-1} - \frac{(n-1)C}{nA} I^{n-2}, \tag{27}$$

with the starting values
$I^0 = \frac{1}{\sqrt{A}} \ln \left| \left(\eta + \frac{B}{2A}\right) + \sqrt{\left(\eta + \frac{B}{2A}\right)^2 + \frac{\Delta}{4A^2}} \right|$, $I^1 = \frac{1}{A} \sqrt{A\eta^2 + B\eta + C} - \frac{B}{2A} I^0.$

Two remaining integrals are evaluated by integration by parts and then using the Euler substitutions: $\sqrt{x_1^2 + x_2^2 + \eta^2} = t + \eta$ for $J_3^s$, and $\sqrt{x_1^2 + (\alpha + \beta\eta)^2 + \eta^2} = t + \sqrt{1 + \beta^2}\eta$ for $J_4^s$.

We conclude that evaluation of singular integrals with polynomial density may be efficiently performed without numerical integration by using the derived recurrent dependences.

*Hypersingular integrals.*
The hypersingular integrals entering (18) contain displacement discontinuities $\Delta u$ as the density. As mentioned, for them we distinguish two cases: (i) when non of triangle apexes is on the fracture contour, and (ii) when one or two apexes are located on the contour.

i) In the first case, we approximate the DD by polynomials. The quadrature rules for this case are given in [10].

ii) For a triangle with an apex on the contour of a fracture, the DD have square-root asymptotics. To increase the accuracy of calculations, it is crucial to account for the asymptotic behavior. For this reason, we approximate the DD by the product of the square-root of the distance from the boundary and a polynomial: $\Delta u = \sqrt{y_i} (x_3 - y_2)^l (x_3 - y_2)^k$, where $i = 1, 2$, $l + k = 0, 1, 2, \ldots, m_p$, $l$ and $k$ are natural numbers, $m_p$ is the degree of the approximating polynomial. It can be shown that all required integrals are reduced to linear combinations of integrals from rational functions, evaluated analytically, and elliptic integrals. We do not dwell on the proof of this statement, which, although straightforward, is lengthy. Rather we focus on the case, which is the most important for practical applications. It is the case, when the square-root factor $\sqrt{y_i}$ is multiplied by a constant.

### 4.3 Hypersingular integrals with square-root and zero order polynomial approximation

Consider the approximation of the DD of the form $\Delta u = \sqrt{y_3}$, which corresponds to a triangle with the side $a$ located on the fracture contour (the side $b$ is orthogonal to the contour). Integration of the hypersingular part of (18) over the triangle, with the DD approximated as explained, shows that the hypersingular integrals are linear combinations of the standard terms:

$$A_{ij} = \frac{\partial^2 A}{\partial x_i \partial x_j}, \; A_{ijk} = \frac{\partial^3 A}{\partial x_i \partial x_j \partial x_k},$$

where $i, j, k = 1, 2, 3$ and $A = \int\limits_{S^q} \frac{\sqrt{y_3} dy_2 dy_3}{\sqrt{x_1^2 + (x_2 - y_2)^2 + (x_3 - y_3)^2}}$.

It can be shown that each of the integrals $A_{ij}$ and $A_{ijk}$ may be expressed in terms of the standard elliptic integrals. From the computational point of view, it is reasonable to use the Carlson elliptic integrals [4]. For instance, after integration over the $y_2$ direction, the term $A_{21}$ is represented by the sum of two elliptic integrals:

$$A_{21} = \int\limits_0^b \frac{x_1 \sqrt{y_3} dy_3}{\left(x_1^2 + \left(x_2 - a + \frac{a y_3}{b}\right)^2 + (x_3 - y_3)^2\right)^{3/2}} - \int\limits_0^b \frac{x_1 \sqrt{y_3} dy_3}{\left(x_1^2 + x_2^2 + (x_3 - y_3)^2\right)^{3/2}}. \quad (28)$$

We evaluate them by using the standard Carlson integral:

$$R_D(x, y, z) = \frac{3}{2} \int\limits_0^\infty \frac{1}{(t + z)\sqrt{(t + x)(t + y)(t + z)}} dt. \quad (29)$$

Then (28) becomes:

$$A_{21} = \frac{2x_1}{3C_1\sqrt{C_1}} \left[ \frac{\varepsilon + \frac{1}{b}}{\varepsilon - \overline{\varepsilon}} R_D\left(\frac{1}{b}, -\overline{\varepsilon}, -\varepsilon\right) + \frac{\overline{\varepsilon} + \frac{1}{b}}{\overline{\varepsilon} - \varepsilon} R_D\left(\frac{1}{b}, -\varepsilon, -\overline{\varepsilon}\right) \right] +$$

$$- \frac{2x_1}{3C_2\sqrt{C_2}} \left[ \frac{\tau + \frac{1}{b}}{\tau - \overline{\tau}} R_D\left(\frac{1}{b}, -\overline{\tau}, -\tau\right) + \frac{\overline{\tau} + \frac{1}{b}}{\overline{\tau} - \tau} R_D\left(\frac{1}{b}, -\tau, -\overline{\tau}\right) \right],$$

where $\varepsilon, \overline{\varepsilon}$ are conjugated roots of the polynomial $A_1 + B_1\left(x + \frac{1}{b}\right) + C_1\left(x + \frac{1}{b}\right)^2$, $A_1 = 1 + \frac{a^2}{b^2}, B_1 = 2(x_2 - a)\frac{a}{b} - 2x_3, C_1 = x_1^2 + (x_2 - a)^2 + x_3^2$, $\tau, \overline{\tau}$ are conjugated roots of the polynomial $A_2 + B_2\left(x + \frac{1}{b}\right) + C_2\left(x + \frac{1}{b}\right)^2$, $A_2 = 1, B_2 = -2x_3, C_2 = x_1^2 + x_2^2 + x_3^2$.

Evaluation of the integral (29) is performed by using the highly efficient technique developed by Carlson. Therefore, we have obtained an efficient means to calculate the influence coefficients accounting for the square-root asymptotics of the DD near a fracture front.

## Acknowledgment

*The authors gratefully acknowledge the support of the European Research Agency (FP7-PEOPLE-2009-IAPP Marie Curie IAPP transfer of knowledge programme, Project Reference # 251475).*

## References

[1] Adachi J., Siebrits E., Peirce A., Desroches J., Computer simulation of hydraulic fractures, Int. J. Rock Mech. Min., 44, 2007, p. 739-757.

[2] Banerjee P. K. and Butterfield R., Boundary element methods in engineering science, McGraw Hill Book Co Ltd., London-New York, 1981, 452 p.

[3] Blinova V. G. and Linkov A. M., A method to find asymptotic forms at the common apex of elastic wedges, J. Appl. Math. Mech., vol. 59 (2), 1995, p. 187-195.

[4] Carlson B. C., A table of elliptic integrals: One quadratic factor, Math. Comput., 1991, 56, p 267-280.

[5] Dobroskok A. A., Linkov A.M., Complex variable equations and the numerical solution of harmonic problems for piecewise - homogeneous media, J. Appl. Math. Mech., vol. 73 (3), 2009, p. 313-325.

[6] Greengard L. and Rokhlin V., A fast algorithm for particle simulations, J. Comput. Phys., vol. 73, 1987, p. 325-348.

[7] Hoenig A., Electric conductivities of a cracked solid, Pure Appl. Geophys., 117, 1978, p. 690-710.

[8] Linkov A. M., Boundary integral equations in elasticity theory, Kluwer Academic Publishers, Dordrecht-Boston-London, 2002, 268 p.

[9] Linkov A. M., Koshelev V. F. and Blinova V. G., Tip, corner and wedge elements: A regular way to increase accuracy of the BEM, Proceedings of IABEM-2002, UT Austin, TX, USA, 2002, CD-ROM.

[10] Linkov A. M., Zoubkov V. V. and Kheib M. A., A method of solving three-dimensional problems of seam working and geological faults, J. Min. Sci., vol. 33 (4), 1997, p. 3-18.

[11] Liu Y. J. and Nishimura N., The fast multipole boundary element method for potential problems: A tutorial, Eng. Anal. Bound. Elem., vol. 30, 2006, p. 371-381.

[12] Mack M. G., Warpinski N. R., Mechanics of hydraulic fracturing. In: Economides M.J., Nolte K.G. (eds) Reservoir simulation, 3-rd edn. John Willey & Sons, 2000, 6.1-6.49.

[13] Rejwer E., Rybarska-Rusinek L. and Linkov A. M., Complex variable Fast Multipole Method for modeling hydraulic fracturing in inhomogeneous media, in Proc. XL Summer School-Conference: APM. Saint Petersburg, Inst. Problems Mech. Engineering, RAS, CD-ROM, 2012, p. 308-314.

*Liliana Rybarska-Rusinek, Dawid Jaworski, Ewa Rejwer, Aleksandr Linkov,*
*Rzeszow University of Technology, Al. Powstancow Warszawy 12, 35-959 Rzeszow, Poland.*